

# Subdiffractive light in bi-periodic arrays of modulated fibers

K. Staliunas<sup>1,2</sup> and C. Masoller<sup>2,3</sup>

<sup>1</sup>*Departament de Física i Enginyeria Nuclear, Universitat Politècnica de Catalunya, Colom 11, 08222 Terrassa, Barcelona, Spain*

<sup>2</sup>*Institució Catalana de Reserca i Estudis Avançats (ICREA), Departament de Física i Enginyeria Nuclear,*

<sup>3</sup>*Institució de Física, Facultat de Ciències, Universidad de la República, Igua 4225 Montevideo 11400, Uruguay*

**Abstract:** We study theoretically the linear and nonlinear propagation of light in one-dimensional bi-periodic arrays of fibers, with the propagation constant periodically modulated along the propagation direction. We predict analytically and observe numerically subdiffractive propagation along such fiber arrays, and characterize the light propagation properties. We also predict novel subdiffractive discrete solitons in the presence of Kerr nonlinearity, both of focusing and defocusing cases, which are essentially different from the usual discrete solitons in waveguide arrays.

©2006 Optical Society of America

OCIS codes: 190.4370, 190.4420, 060.2360

---

## References and links

1. E. Yablonovitch, "Inhibited spontaneous emission in solid-state physics and electronics," *Phys. Rev. Lett.* **58**, 2059 (1987).
2. S. John, "Strong localization of photons in certain disordered dielectric superlattices," *Phys. Rev. Lett.* **58**, 2486 (1987).
3. H. Kosaka, T. Kawashima, A. Tomita, M. Notomi, T. Tamamura, T. Sato and S. Kawakami, "Self-collimating phenomena in photonic crystals," *Appl. Phys. Lett.* **74**, 1212 (1999).
4. D. Chigrin, S. Enoch, C. Sotomayor Torres and G. Tayeb, "Self-guiding in two-dimensional photonic crystals," *Opt. Express* **11**, 1203 (2003).
5. R. Iliew, C. Etrich, U. Peschel, F. Lederer, M. Augustin, H.-J. Fuchs, D. Schelle, E.-B. Kley, S. Nolte, and A. Tünnermann, "Diffractionless propagation of light in a low-index photonic-crystal film," *Appl. Phys. Lett.* **85**, 5854 (2004).
6. D. W. Prather, S. Shi, D. M. Pustai, C. Chen, S. Venkataraman, A. Sharkawy, G. Schneider, and J. Murakowski, "Dispersion-based optical routing in photonic crystals," *Opt. Lett.* **29**, 50-52 (2004).
7. H. S. Eisenberg, Y. Silberberg, R. Morandotti, A. R. Boyd, and J. S. Aitchinson, "Discrete spatial optical solitons in waveguide arrays," *Phys. Rev. Lett.* **81**, 3383 (1998).
8. R. Morandotti, H. S. Eisenberg, Y. Silberberg, M. Sorel and J. S. Aitchinson, "Self-focusing and defocusing in waveguide arrays," *Phys. Rev. Lett.* **86**, 3296 (2001).
9. M. J. Ablowitz and Z. H. Musslimani, "Discrete diffraction managed spatial solitons," *Phys. Rev. Lett.* **87**, 254102 (2001).
10. T. Pertsch, T. Zentgraf, U. Peschel, A. Brauer and F. Lederer, "Anomalous refraction and diffraction in discrete optical systems," *Phys. Rev. Lett.* **88**, 093901 (2002).
11. A. A. Sukhorukov, Y. S. Kivshar, H. S. Eisenberg, and Y. Silberberg, "Spatial optical solitons in waveguide arrays," *IEEE J. Quantum Electron.* **39**, 31-50 (2003).
12. J. Meier, G. I. Stegeman, D. N. Christodoulides, Y. Silberberg, R. Morandotti, H. Yang, G. Salamo, M. Sorel, and J. S. Aitchinson, "Experimental observation of discrete modulational instability," *Phys. Rev. Lett.* **92**, 163902 (2004).
13. T. Pertsch, P. Dannberg, W. Elflein, A. Bräuer, and F. Lederer, "Optical Bloch oscillations in temperature tuned waveguide arrays," *Phys. Rev. Lett.* **83**, 4752 (1999).
14. H. S. Eisenberg, Y. Silberberg, R. Morandotti, and J. S. Aitchinson, "Diffraction management," *Phys. Rev. Lett.* **85**, 1863 (2000).
15. U. Peschel and F. Lederer, "Oscillation and decay of discrete solitons in modulated waveguide array," *JOSA B* **19**, 544 (2002).
16. S. Longhi, M. Marangoni, M. Lobino, R. Ramponi, P. Laporta, E. Cianci, and V. Foglietti, "Observation of dynamic localization in periodically curved waveguide arrays," *Phys. Rev. Lett.* **96**, 243901 (2006).

17. K. Staliunas and R. Herrero, Nondiffractive propagation of light in photonic crystals, *Phys. Rev. E*, **73**, 016601 (2006).
18. K. Staliunas, R. Herrero and G. J. de Valcarcel, Sub-diffractive band-edge solitons in Bose-Einstein condensates in periodic potentials, *Phys. Rev. E* **73**, 065603(R) (2006).

## 1. Introduction

The ability to realize an optical medium in which light propagates without diffraction would have important implications for today's fiber-optic-based telecommunications. It was recently shown that photonic crystals (PCs) can provide a mean for achieving this goal. The PCs, in addition to their well known properties of manipulating the temporal dispersion, i.e. of introducing the band gap for the light propagation [1, 2], were recently shown to be able to manipulate the spatial dispersion (diffraction) properties [3-6]. While circular sectors in dispersion curves (the iso-frequency lines in the wavevector space) indicate the normal dispersion, and convex segments in these curves indicate negative diffraction, the "flat" segments that arise for specific PCs architectures, indicate zero diffraction (or more precisely sub-diffraction, as the first-order diffraction term vanishes for frequencies within the flat segments, but higher-order terms remain).

In this Letter we describe the sub-diffractive propagation of light in a one-dimensional array of coupled waveguides. The scheme of the fiber array proposed here aims to imitate the phenomena occurring in sub-diffractive photonic crystals, i.e., we consider a modulated fiber array whose structure is similar to that of sub-diffractive PCs. The key ingredient of our scheme is that the propagation constant in the fibers is modulated along the longitudinal (propagation) direction. One can implement the modulation of the propagation constant by periodically changing the thickness of the individual fibers in an alternating order, as depicted in Fig. 1. The periodic variation of the propagation constant along the  $z$ -direction can also be obtained by fine temperature control, or it can be realized modifying directly the refractive index of the fibers (incorporating in the fibers periodic profiles of impurities). The fabrication and manipulation of these structures at the nanoscale is nowadays possible using, e.g., lithography.

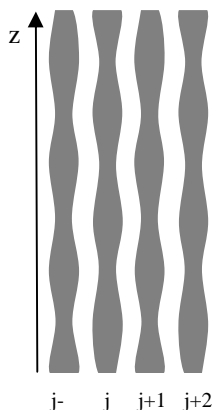


Fig. 1. Qualitative representation of the modulated fiber array. The grey regions indicate the thickness of the fibers. Notice the alternating periodic variation of the thickness along the  $z$ -direction: for values of  $z$  such that the thickness of the fiber  $j$  is maximum, the thickness of the neighboring fibers,  $j-1$  and  $j+1$ , is minimum. It can be also observed that the distance between the cores of the fibers is constant along the  $z$ -direction.

The main aim of our work is the demonstration of linear sub-diffractive propagation of light in such modulated fiber array. In addition we study the influence of the Kerr nonlinearity, and demonstrate the sub-diffractive propagation as well as formation of soliton-like localisations. Recently, there has been a lot of interest in diffraction management in

discrete systems and the so-called discrete solitons [7-12]. The soliton-like structures reported here resemble those found in Refs. [7-12], in the sense that they reside in nonlinear fiber arrays. However, they originate from different physical mechanisms: while the discrete solitons reported previously rely on the interplay of focusing/defocusing and positive/negative diffraction, the solitons reported here appear at regions of zero diffraction (more precisely, at flat segments of the spatial dispersion curve, where the first-order diffraction term vanishes).

The modulated fiber array that we propose also has similarities with the fiber arrays proposed in Refs. [13-16], inspired in diffraction management in photonic crystals, and exploiting the fact that diffraction vanishes for specific values of the propagation constant. In Ref. [15] Peschel and Lederer proposed a longitudinal periodic variation of the coupling constant, while in Ref. [16], Longhi considered sinusoidally curved arrays. The advantage of the configuration proposed here is that it allows eliminating not only the first-order diffraction (second order spatial derivatives), but due to symmetry, also all the odd-order derivatives. The remaining terms can be approximated, at the lowest order, by the fourth-order spatial derivative (recently, a similar effect was shown to happen in symmetric PC [17]), and allows the existence of localized soliton-like solutions, similarly as in symmetric nonlinear PCs, and in Bose-Einstein condensates in periodic in space and in time potentials [18].

In the first part of this Letter we present analytic results that demonstrate the existence of regimes of sub-diffractive linear propagation. We calculate the spatial dispersion, and show the formation of the flat segments of the dispersion curves: the light with wavevector within these segments propagates sub-diffractively. Next we present results of numerical simulations: we characterize the sub-diffractive linear regime in the parameter space of coupling strength, and modulation depth. In the third part of the Letter we show the possibility of sub-diffractive discrete solitons in the nonlinear case (with both types of Kerr nonlinearities, of the focusing and defocusing sense), followed by conclusions.

## 2. Model

We consider the scheme depicted in Fig. 1, where the propagation constant in the  $j$ -th fiber is given by:

$$\beta_j(z) = \beta_0 + 2\Delta\beta(-1)^j \cos(qz), \quad (1)$$

where the factor  $(-1)^j$  is responsible for the alternating character of the longitudinal modulation,  $j=1,2,\dots,N$ , is the fiber number,  $\Delta\beta$  is the modulation depth, and  $q$  is the longitudinal modulation wavenumber, which without loss of generality we consider equal to unity throughout the paper, since the longitudinal coordinate  $z$  is re-scaled as:  $zq \rightarrow z$  below. In the slow varying envelope approximations and assuming single-mode fibers, the equations describing light propagation in the  $j$ -th fiber read:

$$\frac{dA_j}{dz} = i \cdot 2\Delta\beta(-1)^j \cos(z)A_j + ic(A_{j-1} + A_{j+1}) + i\gamma|A_j|^2 A_j, \quad (2)$$

where  $A_j$  is the complex amplitude of the field in the  $j$ -th fiber,  $c$  is the strength of the coupling between the neighbouring fibers, as occurs through the overlapping evanescent fields, and  $\gamma$  is the strength of the Kerr nonlinearity, which is considered to be focusing if  $\gamma > 0$  and defocusing if  $\gamma < 0$ . In Eq. (2) the amplitudes  $A_j$  and the parameters are dimensionless. The procedure for deriving Eq. (2) from the discrete nonlinear Schrodinger equation, as well as the normalisations of field amplitudes and constants in Eq. (2) is the same as that described in Ref. [15]. The transverse coordinate, in addition, is normalized to the distance between the neighbouring fibers, and the longitudinal coordinate, to the inverse wave number of longitudinal modulation  $q^{-1}$ . In general  $c$  and  $\gamma$  might also be modulated along the

array of fibers and/or along the propagation direction, depending on the specific fabrication details. Because we consider weak modulation,  $\Delta\beta \ll \beta$ , and because the distance between the core of the fibers is constant along the array and along the propagation direction, we neglect all variations of  $c$  and  $\gamma$ .

First we investigate the linear propagation of light when  $\gamma=0$ . We look for a probe solution in the form of a discrete Bloch mode:

$$A_j = e^{ikz} e^{i \cdot j \Delta\varphi} \sum_{n=-\infty}^{\infty} (-1)^{j \cdot n} a_n e^{inz}, \quad (3)$$

Here  $k$  is the wavevector of the Bloch mode,  $\Delta\varphi$  is the phase shift between the light fields between the neighbouring fibers in the Bloch mode (corresponds to the tilt of the mode),  $a_n$  is the complex amplitude of  $n$ -th (longitudinal) harmonics of the Bloch mode ( $a_0$  is the amplitude of the homogeneous component, and  $a_{\pm 1}$  are the amplitudes of the most significant first harmonics of the Bloch mode). The odd Bloch mode components have the alternating shape across the fiber array, which is considered by the factor  $(-1)^{j \cdot n}$  in Eq. (3). Substituting Eq. (3) in Eq. (2), collecting the same exponents of the longitudinal harmonics, we obtain the following system of coupled equations for the harmonic components:

$$i(k+n)a_n = i\Delta\beta(a_{n-1} + a_{n+1}) + 2ic(-1)^n \cos(\Delta\varphi)a_n \quad (4)$$

### 3. Linear subdiffractive propagation

To solve Eq. (4) we have to truncate this system, i.e., to keep a certain, finite number of harmonics. Figure 2 displays a particular solution of Eq. (4), obtained by truncating to three lowest harmonics  $n = -1, 0, +1$ , which is in fact the spatial dispersion curve  $k(\Delta\varphi)$  of the Bloch modes.

The appearance of the horizontal plateaus in the dispersion curves shown in Fig. 2 indicates the existence of regimes of subdiffractive propagation. Indeed, these plateaus mean that the longitudinal wavevectors  $k$  of the corresponding Bloch mode do not depend on  $\Delta\varphi$ , i.e., that the components that are tilted at different angles do not dephase during the propagation. This means that the beam (or any arbitrary pattern), being a Fourier composition of differently tilted components of Bloch modes, does not broaden or blur during the propagation. (Obviously, there are high-order terms of diffraction that do not vanish, as investigated below, therefore, we refer to subdiffractive- rather to nondiffractive propagation).

The appearance of plateaus at  $\Delta\varphi \approx 0$  is essentially the result of the interaction of two uncoupled dispersion curves, those with  $n = -1, 0$ , as can be seen from the Fig. 2 (the plateaus at  $\Delta\varphi \approx \pm\pi$  result from the interaction of the other two curves  $n = 1, 0$ ), as the disshaping (lift of degeneracy) of the dispersion curves occurs at (and due to-) the cross of two dispersion curves. As we focus on the case  $\Delta\varphi \approx 0$ , this allows the truncation of the system of equations (4) to only two Bloch modes in the limit of  $\Delta\varphi \approx 0$ . This leads to simple and useful analytical predictions. The truncated system reads:

$$ika_0 = i\Delta\beta a_{-1} + 2ic \cos(\Delta\varphi) a_0, \quad (5a)$$

$$i(k-1)a_{-1} = i\Delta\beta a_0 - 2ic \cos(\Delta\varphi) a_{-1}. \quad (5b)$$

The eigenvalues of Eq. (5) read:

$$k(\Delta\varphi) = \frac{1}{2} \pm \frac{1}{2} \sqrt{4\Delta\beta^2 + (1 - 4c \cdot \cos(\Delta\varphi))^2}, \quad (6a)$$

and the associated eigenvectors:

$$\left( -1 + 4c \cdot \cos(\Delta\varphi) \pm \sqrt{4\Delta\beta^2 + (1 - 4c \cdot \cos(\Delta\varphi))^2}, \quad 2\Delta\beta \right). \quad (6b)$$

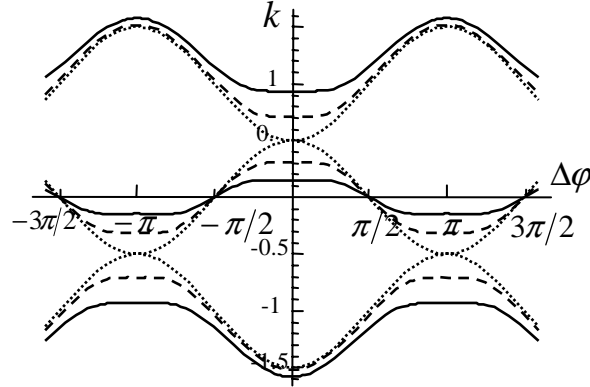


Fig. 2. Spatial dispersion curve obtained by solving Eq. (4) truncated to three modes. The wavenumber is plotted vs. the tilt of the Bloch modes. The dotted curves correspond to the limit of small modulation,  $\Delta\beta \rightarrow 0$ , when the three equations become uncoupled. The parameters are  $c = 0.25$ ,  $\Delta\beta = 0.2$  (dashed) and  $\Delta\beta = 0.4$  (solid), and correspond to the case when the uncoupled curves just touch one another. In this situation, an increase of the modulation depth  $\Delta\beta$  broadens the subdiffractive plateau.

Equation (6) allows us to explore analytically the basic regimes of the propagation. The condition for the appearance of the flat segments (zero curvature plateaus),  $\partial^2 k / \partial \Delta\varphi^2 = 0$ , is fulfilled for  $c = 0.25$  and for the arbitrary values of the modulation amplitude  $\Delta\beta$ , as can be easily found from Eq. (6a). A variation of  $\Delta\beta$  results in a change in the width of the plateau only, as can be anticipated from Fig. 2. The half-width of the plateau, evaluated from Eq. (6), is  $\Delta\varphi_{\text{plateau}} \approx 2\sqrt{\Delta\beta}$ . Another interesting point is that there are two plateaus (see Fig. 2). The plateaus of the dispersion curves are separated at  $\Delta\varphi = 0$  by  $2\Delta\varphi_{\text{sep}} = 2\Delta\beta$  as follows easily from Eq. (6a). In the case of subdiffractive PCs, where only one plateau has been found [17], the initial beam projects essentially on two modes – diffractive and subdiffractive. The first one diffracts quickly and vanishes, while the second one continues to propagate collimated. Here, the initial beam projects into two sub-diffractive modes, which propagate together without broadening (there is actually a weak, subdiffractive broadening evaluated below). As these two modes have different propagation constants a “beating”, i.e., periodic pulsations with respect to the longitudinal coordinate, can be expected. These pulsations are clearly seen in the simulations presented below.

Summarizing: the analysis based on Eq. (5) and Eq. (6) allowed to calculate analytically:

(i) the minimum half-width of nondiffractive beam,  $\Delta x \approx 2\pi / \Delta\varphi_{\text{plateau}} = \pi / \sqrt{\Delta\beta}$  as follows from the width of the plateau. When the initial beam is narrower than the minimum width, then the beam rapidly recovers the minimum width  $\Delta x$ , and continues to propagate with a weak subdiffractive spreading as governed by the second order diffraction;

(ii) The character of the sub-diffraction at zero diffraction point  $c = 0.25$  is described by the next, non-vanishing order derivative of the dispersion relation. As the third order derivative vanishes, due to the symmetries, the fourth order derivative becomes dominating. The second order diffraction is:  $d_4 = (1/4!) \partial^4 k / \partial \Delta \varphi^4 = 1/(24\Delta\beta)$ , and can be used to evaluate weak spreading in the long range propagation as in [17] for the case of photonic crystals.

(iii) The spatial period of the beat is  $\Delta z \approx 2\pi/\Delta k_{sep} = 2\pi/\Delta\beta$  as follows from the separation of the dispersion curves. The initial Gaussian beam projecting into two modes results in a spatial beat. Especially prepared initial beams, corresponding to the envelopes of the eigenvectors of the Bloch modes (6), propagate steadily, without the beat. At the zero diffraction point  $c = 0.25$  and for the almost parallel propagation,  $\Delta\varphi \approx 0$ , the eigenvectors (6b) simplify to:  $(\pm 1, 1)$ , which means 100% modulation of the fields.

Next we present results of numerical simulations of Eq. (2), in order to check the above analytical predictions. We consider an array of  $N=120$  fibers with periodic boundary conditions. Figure 3 displays the width of the final beam (after propagating a distance  $L=100$ ) in the parameter space  $(c, \Delta\beta)$  (the width is normalized to  $\sqrt{c}$ ). The initial condition is a Gaussian beam of half-width  $\Delta x = 3$  (normalized to the distance between the fibers). The color scale is such that the red regions correspond to large-, and blue- to small, final width of the beam (obviously always larger than the initial beam). A clear region of subdiffraction propagation for  $c = 0.25$  can be observed, in a good agreement with the above analysis. (We note that the analytic expressions are valid for  $\Delta\beta \ll 1$ .) For the moderate modulation depth ( $\Delta\beta \geq 0.3$ ) the minimum width is obtained for coupling values different from the predicted value,  $c = 0.25$ . In addition, another sub-diffractive branch can be observed at larger  $c$ , absent in the analytical treatment when the expansion (3) is truncated to two or three Bloch modes, but that can be found when at least 5 modes are included in the expansion.

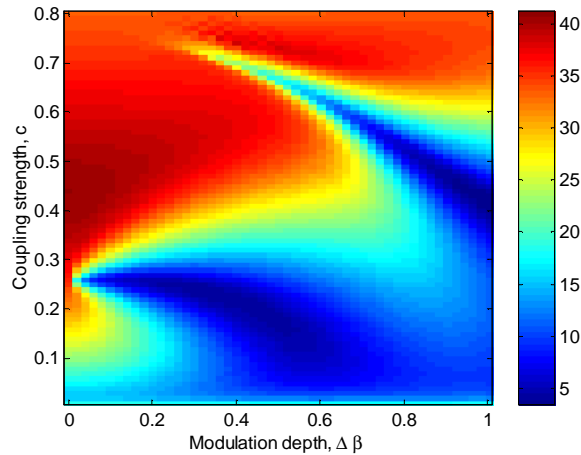


Fig. 3. The width of the beam in the parameter space  $(c, \Delta\beta)$  as obtained by numerical integration of (2) over propagation distance of  $L=100$ , and starting from initial Gaussian beam. The color scale is such that the red regions correspond to large-, and the blue- to small final width of the beam.

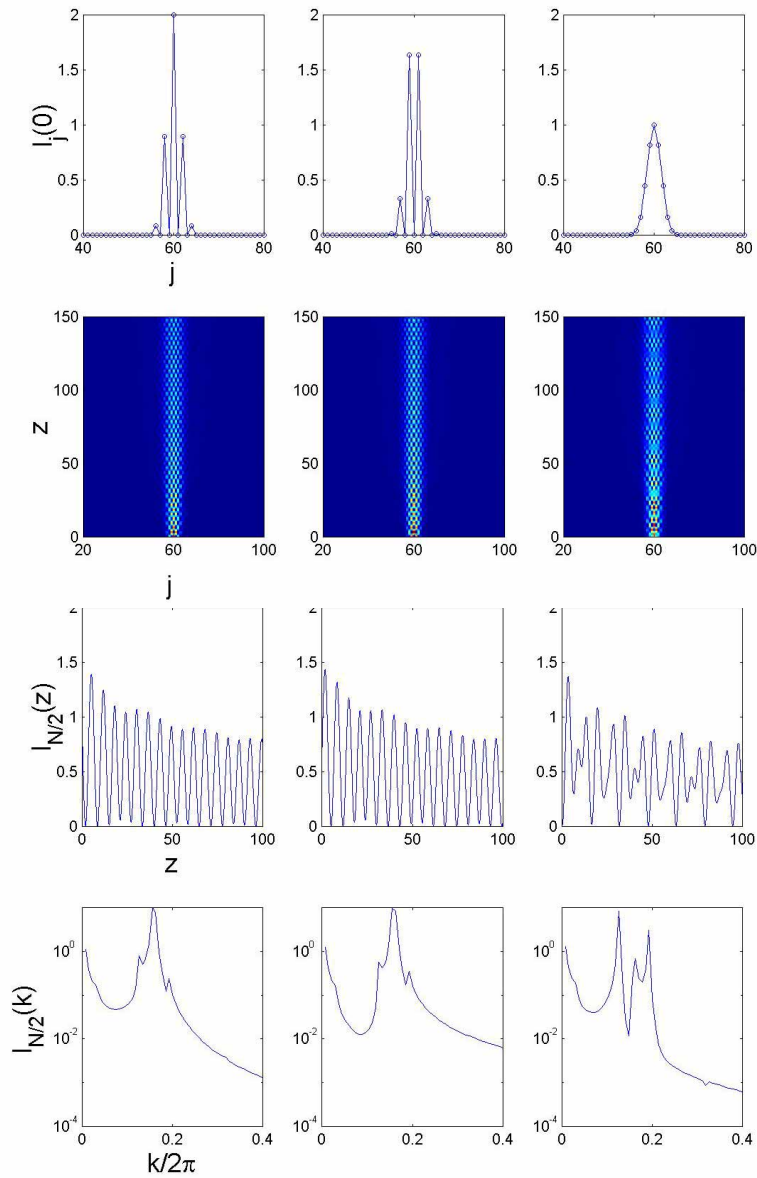


Fig. 4. Sub-diffractive propagating of beams, as obtained by numerical integration of (2) with  $c=0.25$  and  $\Delta\beta=0.1$ . The top row displays the initial condition, the second row displays the density plots of the beam propagation, the third row displays the evolution of the intensity in the central fiber, and the bottom row - the Fourier power spectra of the intensity evolution. Different columns correspond to different initial conditions: left column – envelope of the  $(1,1)$  Bloch mode; Middle column – envelope of  $(-1,1)$  Bloch mode. Right column – Gaussian beam, with eigenvector  $\begin{pmatrix} 1,0 \end{pmatrix}$ , which can be considered as a combination of the Bloch modes:  $\begin{pmatrix} 1,0 \end{pmatrix} = \frac{1}{2}(\begin{pmatrix} 1,1 \end{pmatrix} - \begin{pmatrix} -1,1 \end{pmatrix})$

Typical examples of sub-diffractively propagating beams are given in Fig. 4. The density plots represent the beams spreading much less than those in arrays of homogeneous fibers. We note that the analog of the Rayleigh length (the distance at which the beam spreads by the factor of  $\sqrt{2}$ ) for the array of not modulated fibers  $\Delta\beta = 0$  is  $L_R = \Delta x^2 / (2c)$ , which for the given conditions results in  $L_R \approx 20$ . The shapes of the entering beam are also indicated in the Fig. 4. They are either the Gaussian beam, or the envelopes of the two Bloch modes with eigenvectors  $(\pm 1, 1)$ , as following from (6b).

According to the expectations, the envelopes of the pure Bloch modes propagate almost without oscillations in the longitudinal direction. Dominating oscillations of spatial period of  $2\pi$  of the longitudinal modulation are pronounced in the temporal plots as well as the Fourier power spectrum in Fig. 4. In fact the weak oscillations are also visible as weak sidebands, due to not exact matching with the “true” Bloch mode (appearing in the infinite expansion of (3)). The Gaussian input, however, results into pronounced “beats” along the propagation direction, since the initial Gaussian beam projects nearly equally into two nondiffractive Bloch modes with different propagation constants. The calculation of this beat period are in a quantitative agreement with analytics:  $\Delta z \approx 2\pi / \Delta k_{sep} = 2\pi / \Delta\beta$ .

#### 4. Sub-diffractive solitons

After demonstration of the sub-diffractive propagation of the beams in the linear case, we consider the nonlinear propagation with the Kerr nonlinearity. Exactly at the zero diffraction point one can expect the spatial solitons for defocusing Kerr nonlinearity, in analogy to the continuous case [18]. These solitons are the stationary envelopes of the particular Bloch mode, where the second order diffraction (fourth order derivative) is compensated by the nonlinearity. However, differently from [18] where the solitons occur only for defocusing Kerr nonlinearity (as compensating the second order diffraction of positive sign), the solitons here can occur for both types of nonlinearity. For defocusing nonlinearity the solitons would involve the radiation on one Bloch mode (with the positive sign of the second order diffraction), and for the focusing nonlinearity – on the other mode.

The results of numerical integration indeed show that expected result. An attempt to generate solitons as the envelopes of the Bloch modes with the “wrong” combination of the signs of nonlinearity and diffraction does not lead to soliton solution (cases (a) and (e) in Fig. 5). The correct combination of signs, (b) and (d), corresponds to self-trapping into solitons. Finally, the initial Gaussian beam leads to the transient selection: half of radiation projecting into the “wrong” Bloch mode diffracts away, and the other half, projecting into the “correct” mode, self-traps into the soliton-type beam and propagates steadily along the array of fibers. The latter phenomena, we note, occurs for the both signs of the nonlinearity [cases (c) and (f) in Fig. 5].

In order to check the conclusions of the nonlinear soliton propagation we integrated (2) over long propagation distances, and filtered out the outgoing radiation at the boundaries of the integration region in the transient stages of the solitons formation. We found that: i) the shapes reached the stationary state after the transient evolution (apart from the small scale oscillations of the Bloch mode) and ii) the width and the amplitude of the solitons depend on the initial conditions, which indicates at least one parameter family of soliton-type solutions. The detailed investigation of the solitons properties fall out of the scope of the article, and will be presented elsewhere.

#### 5. Conclusions

Concluding, we demonstrated the sub-diffractive propagation of light in one-dimensional arrays of fibers, which have their index of refraction periodically modulated along the propagation direction in the alternating order. We calculated analytically the main characteristics of the propagation: the minimum width of the beam, the asymptotic broadening, and the spatial beat between two nondiffractive Bloch modes, and we checked



these conclusions by numerical integration of the full model equations. We also analyzed the influence of Kerr nonlinearity and found sub-diffractive discrete solitons for both, focusing and defocusing nonlinear terms. The solitons reported here are nonlinear localizations which differ from previously reported discrete solitons because they are based on the *second-order diffraction*, and not on the first one (positive or negative) as usual. Therefore, it can be expected that they scale differently (this study is in progress and will be reported elsewhere). In addition, due to the simultaneous presence of several dispersion curves, the sub-diffractive solitons can occur on one of two possible branches for a given nonlinearity, and in this sense they also differ from previously reported discrete solitons. Concerning the level of optical power required for soliton generation, we speculate that the intensities are significantly smaller than those for needed for usual discrete solitons. Because the solitons in general are formations where nonlinearity balances the dispersive-diffractive spreading, and in our case diffraction is very weak (sub-diffraction), it can be expected that a weaker nonlinearity is required for this balance. Concerning the type of fiber needed, the same type of fibers (but modulated) are to be used in our proposal as those that have been used in previous studies.

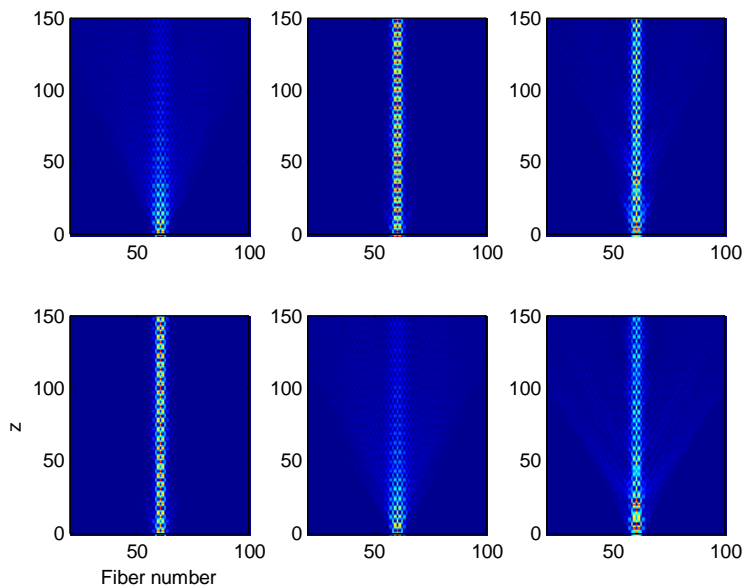


Fig. 5. Sub-diffractive propagation in the presence of positive and negative nonlinearities ( $\gamma = 0.1$  in the top row,  $\gamma = -0.1$  in the bottom row, other parameters and initial conditions as in Fig. 4).

### Acknowledgments

The work was supported by Spanish Ministerio de Educación y Ciencia through project FIS2005-07931-C03-03. C. Masoller also acknowledges support from the “Ramon and Cajal” Program (Spain).